

pubs.acs.org/acsapm Letter

Tissue-Mimetic Dielectric Actuators: Free-Standing, Stable, and Solvent-Free

Vahid Karimkhani, Mohammad Vatankhah-Varnosfaderani,* Andrew N. Keith, Erfan Dashtimoghadam, Benjamin J. Morgan, Michael Jacobs, Andrey V. Dobrynin, and Sergei S. Sheiko*



Cite This: ACS Appl. Polym. Mater. 2020, 2, 1741-1745



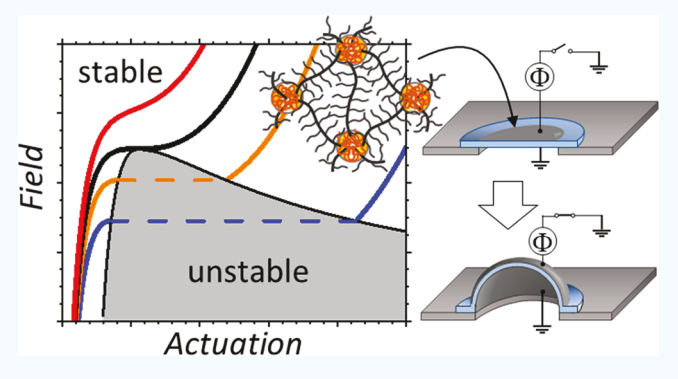
ACCESS

III Metrics & More

Article Recommendations

SI Supporting Information

ABSTRACT: One of the notorious problems in dielectric elastomer actuators (DEAs) is electromechanical instability resulting in uncontrolled breakdown, which precludes large reversible strokes. We resolved this issue by using thermoplastic elastomers (plastomers) self-assembled from linear-bottlebrushlinear triblock copolymers composed of poly(methyl methacrylate) linear blocks and polydimethylsiloxane brush blocks. These materials demonstrate a unique combination of initial softness and intense strain-stiffening at larger deformations, which is analogous to the signature behavior of biological tissues. Plastomer-based free-standing DEAs operate at low electric fields ($\sim 1~V/\mu m^{-1}$) and enable large (5-fold) reversible strokes. Given the excellent thermal stability and hydrophobicity of silicone, these



solvent-free materials are good candidates for the design of artificial muscles and are capable of operating in a broad range of environments, including the human body and ocean, without losing actuation performance.

KEYWORDS: dielectric elastomer actuators, bottlebrushes, thermoplastic elastomers, strain-stiffening, self-assembly

S oft robots of the future require emulating the characteristic performance of adaptable biological actuators like an octopus' arm or an elephant's trunk. This includes replication of both biological mechanics (inherent softness, strain-adaptive stiffening, and strength) and efficient actuation with fast responses under large strokes. Current dielectric elastomer actuators (DEAs) meet some of these requirements as artificial muscles due to their quick (\sim 1 kHz), efficient (work density \sim 10³ J/kg), and significant (\sim 100%) dimensional changes when subjected to electric fields (Figure 1a). However, these often require high electric fields (>10 V/ μ m) and suffer from electromechanical instability (EMI), also known as snap-through instability, which leads to uncontrolled electrical or mechanical breakdown (EBD or MBD). The goal of this study was to develop a new materials design platform that would deliver DEA materials without an inherent EMI.

This instability is a manifestation of the DEA equilibrium state, which is determined by a balance of the mechanical (σ_{true}) and Maxwell stresses (P) generated in an elastomer film compressed from its initial thickness h_0 to h under an applied voltage Φ (Figure 1a) as

$$\sigma_{\text{true}}(\lambda) + \varepsilon_0 \varepsilon (\Phi/\lambda h_0)^2 = 0 \tag{1}$$

where $\lambda = h/h_0$ is the deformation ratio, $\varepsilon_0 = 8.85 \times 10^{-12} \text{ F}$ m⁻¹ is the vacuum permittivity, and ε is the relative dielectric

constant of the elastomer. The mechanical stress of elastomeric materials undergoing uniaxial deformation at constant volume is given by the following equation of state:

$$\sigma_{\text{true}}(\lambda) = \frac{E}{9} (\lambda^2 - \lambda^{-1}) \left[1 + 2 \left(1 - \frac{\beta(\lambda^2 + 2\lambda^{-1})}{3} \right)^{-2} \right]$$
(2)

where E is the structural Young's modulus determined by network cross-link density and strain-stiffening parameter $\beta = R_{\rm in}^2/R_{\rm max}^2$, which characterizes the nonlinear modulus increase due to extension of the network strands from their initial mean-square end-to-end distance $R_{\rm in}^2$ to their maximum contour length $R_{\rm max}$ such that $0 < \beta < 1.^{12-14}$ Flexible linear-chain elastomers and gels ($R_{\rm in} \ll R_{\rm max}$) display weak strain stiffening behavior with $\beta \cong 0.01-0.1$, while networks with semiflexible strands ($R_{\rm in} \sim R_{\rm max}$) are characterized by a higher values of the parameter $\beta \approx 0.1-1.^{15}$ Note that for flexible

Received: February 9, 2020 Accepted: April 1, 2020 Published: April 1, 2020





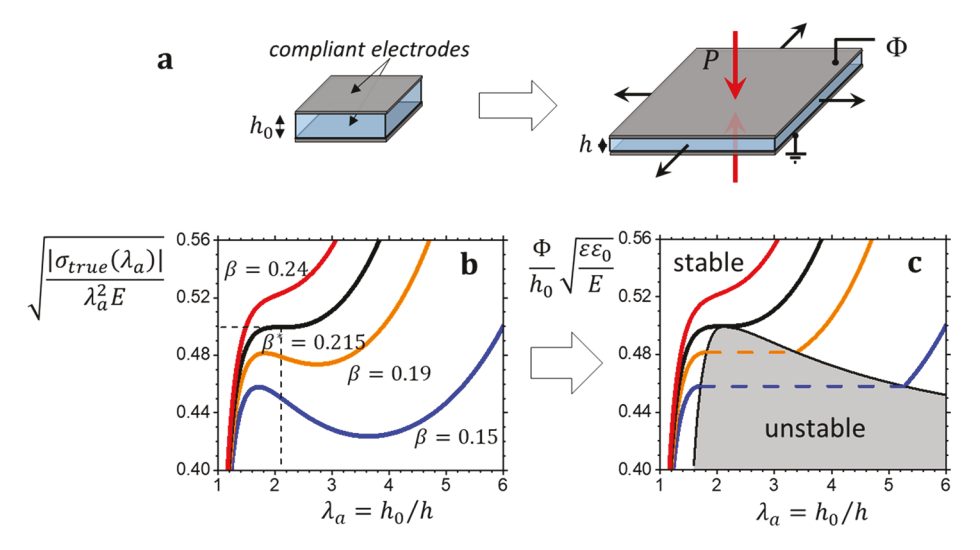


Figure 1. (a) A dielectric elastomer film between two compliant electrodes undergoes uniaxial compression from initial thickness h_0 to h upon applying a voltage Φ . At equilibrium, the Maxwell stress $P(\lambda)$ is balanced by the mechanical stress $\sigma_{\text{true}}(\lambda)$ generated in compressed elastomer (eq 1). (b) Dependence of the r.h.s. of eq 3 on λ_a for different values of the parameter β . (c) Diagram of states for DEA in terms of the dimensionless parameter $\sqrt{(\varepsilon_0 \varepsilon/E)} \Phi/h_0$ and areal deformation ratio λ_a for different values of the parameter β . Dashed lines show a snap-through film compression in the unstable region colored in gray due to the EMI.

strands with $\beta \rightarrow 0$, eq 2 simplifies to its conventional form as $\sigma_{\text{true}}(\lambda) = E(\lambda^2 - \lambda^{-1})/3.^{16}$

By combining 1, we transform deformation curves of elastomer films (Figure 1b) into actuation curves (Figure 1c) in terms of dimensionless variables where $\lambda_a = \lambda^{-1} = h_0/h$ is the areal extension ratio.

$$\sqrt{(\varepsilon_0 \varepsilon / E)} \Phi / h_0 = \lambda_a^{-1} \sqrt{\frac{|\sigma_{\text{true}}(\lambda_a)|}{E}}$$
(3)

This representation allows describing film deformation in universal form in terms of the strain-stiffening parameter β . The EMI follows from the functional form of the right hand side (r.h.s.) of eq 3, which could be considered as a two-valued function of λ_a for β < 0.215 and single-valued function in the interval $\beta \ge 0.215$, as shown in Figure 1b. Correspondingly, eq 3 solutions can also be represented as a diagram of stable and unstable regions with a snap-through instability at β < 0.215 and stable actuation in the entire applied voltage interval by elastomers with $\beta > 0.215$ (Figure 1c).

Various DEA systems have been proposed to overcome EMI, yet limit their applicability by trading off either efficiency or free-standing capability. 17-21 However, synthesizing materials with enhanced softness, strain-stiffening, dielectric constant, and strength affords an opportunity for inherent elimination of these shortcomings. 10,11,13,22-25 Unfortunately, many cutting edge DEA material designs are based on various types of gels that are prone to spontaneous evaporation, vitrification upon cooling, and leakage under deformation. Therefore, we look to two elastomeric material platforms based on solvent-free brush-like architecture for guidance: (i) chemically crosslinked elastomers (Figure 2a)²⁶ and (ii) physically cross-linked plastomers (Figure 2b)²⁷ both of which possess distinct stress-strain responses (Figures 2c-f) that suggest favorable actuation behaviors (Figures 2g, h). It follows from Figure 2c, d that a unique feature of the brush architecture is the ability to program both Young's modulus (stress-strain slope at small deformation)

$$E_0 \equiv \lim_{\lambda \to 1} \frac{3\sigma_{\text{true}}(\lambda)}{\lambda^2 - \lambda^{-1}} = \frac{E}{3} (1 + 2(1 - \beta)^{-2})$$
(4)

and β by varying three architectural parameters-side chain length (n_{sc}) , grafting density (n_g^{-1}) , and strand length (n_x) , where n_g is degree of polymerization of backbone spacer between neighboring side chains. ²⁶ In terms of these mechanical characteristics, System 1 demonstrated superior combinations of softness $(E_0 \cong 10^3 - 10^5 \text{ Pa})$ and strain stiffening ($\beta = 0.08-0.28$) beneficial for DEA (Figure 2c). ¹⁴ This solvent-free strain-stiffening response was on par with swollen polymer gels; however, it was short of completely precluding EMI especially when targeting low-voltage supersoft DEAs with $E_0 \sim 10^3$ Pa (Figure 2g). However, given the control parameters (n_{sc} and n_x), it is increasingly difficult to synthesize elastomers with $\beta > 0.2$ as it requires very long side chains and very short backbones between cross-links. In addition, both approaches would severely limit the operational range for actuation strokes due to the upper bound on the extensibility at $\lambda_{\max} \cong \beta^{-0.5} \cong 2$. Exploring physical networks of self-assembled linear-bottlebrush-linear (LBL) triblock copolymer plastomers (System 2)^{27,28} could completely eliminate EMI and enable full actuation control. In contrast to chemically cross-linked elastomers, the brush-like strands with the same $n_{\rm sc}$ = 14 are significantly more extended and therefore exhibit a much stronger strain-stiffening response (Figure 2d). As verified by atomic force microscopy and X-ray scattering measurements, ^{27,29} this behavior is a product of the strong microphase separation between both chemically and architecturally distinct blocks, which strongly drives network strands into the nonlinear finite extensibility regime, resulting in increasingly nonlinear stress-strain responses. 13,15 Even with constant bottlebrush block dimensions (n_{bb} , n_{sc}), the mechanical response of plastomers is largely controlled by degree of polymerization of the liner block (n_L) , which determines the aggregation number and hence cross-linking functionality. Furthermore, plastomers exhibit a characteristic S-shape in differential modulus plots $(\partial \sigma_{true}/\partial \lambda)$ due to sequential nonlinear elastic compliance followed by micro-

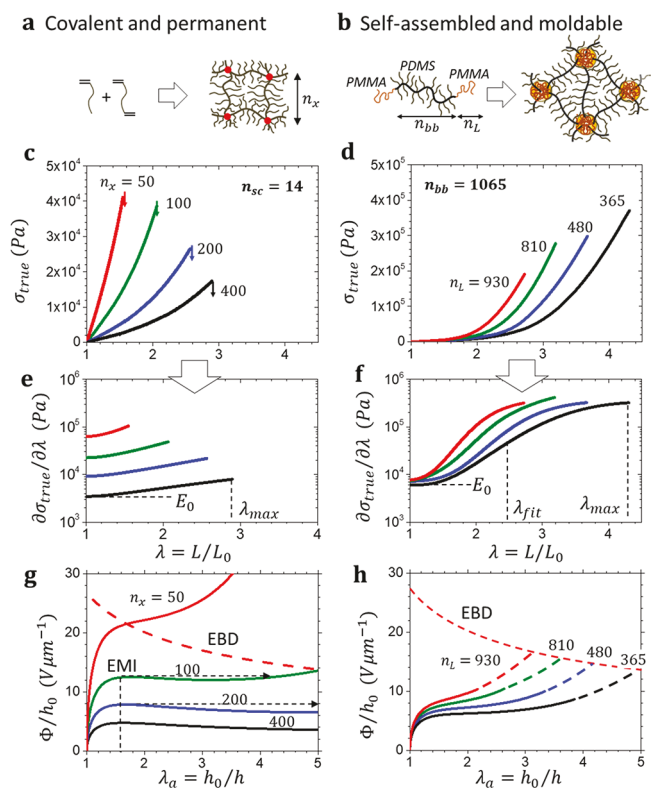


Figure 2. Architectural control of mechanical and electroactuation properties. (a, b) Formation schematics of covalent (System 1) and physical (System 2) polymer networks with brush-like strands. (c, d) True stress vs uniaxial elongation $\lambda = h_0/h$ curves of System 1 and System 2. In elastomers (System 1) with polydimethylsiloxane (PDMS) side chains $n_{sc} = 14$, the stress-strain response is controlled by backbone degree of polymerization between cross-links (n_x) . In plastomers with PDMS side chains (System 2) with constant brush block dimensions ($n_{bb} = 1065$ and $n_{sc} = 14$), degree of polymerization of the linear blocks n_L largely dictates strain-stiffening β . (e, f) Plotting differential modulus $\partial \sigma_{\text{true}}/\partial \lambda$ as a function of λ highlights plastomers characteristic S-shape analogous to the strain-stiffening behavior of soft biological tissues. (g, h) Electric field as a function of areal expansion $\lambda_a = \lambda^{-1}$ is calculated from the mechanical curves in (c, d) plotted with electric field $\Phi/h_0=\lambda_{\rm a}^{-1}\sqrt{|\sigma_{\rm true}(\lambda_{\rm a})|/\varepsilon_0\varepsilon}$, where $\varepsilon=2.94$ ± 0.02 is the relative dielectric permittivity of bottlebrush PDMS. 14 Unlike elastomers, plastomers preclude EMI, displaying continuously increasing Φ/h_0 and enabling higher strokes as quantified by λ_a and controlled by $n_{\rm L}$.

domain yielding at larger strains (Figure 2f), which is analogous to the deformation hierarchy of tissue's collagen networks. In sum, while both systems are able to achieve tissue relevant softness ($E_0 \cong 10^3$ Pa), only bottlebrush plastomers (System 2) enable sweeping control of strain stiffening ($\beta = 0.2-0.7$) and the resulting stable actuation (Figure 2h).

To further investigate this, we synthesized an LBL plastomer series (Table 1) with constant bottlebrush block dimensions and systematically increased linear block length. We scale up our previous synthesis²⁷ to afford large volume of materials with enhanced strain-stiffening parameters beyond the theoretical EMI threshold of $\beta^* = 0.215$. The unique combination of plastomer softness ($E_0 \cong 1-10$ kPa) and strain stiffening ($\beta \cong 0.3-0.6$) empowers freestanding, EMI-free, and controlled reversible electroactuation of thick ($h_0 \sim 1$ mm) films over broad deformation ranges (Figure 3). The softest

Table 1. Molecular Parameters and Mechanical Properties of Plastomers

sample	$n_{\rm bb}^{a}$	$n_{\rm L}^{}$	$\phi_{\scriptscriptstyle m L}{}^{c}$	$\lambda_{\mathrm{fit}}^{}d}$	E^e	eta^f	E_0^{g}	E_0^h
900-1	884	145	0.03	2.1	1600	0.27	2550	2900
900-2	884	438	0.08	1.8	1850	0.39	3900	4300
900-3	884	667	0.11	1.7	2850	0.49	8200	7650
900-4	884	867	0.14	1.6	2000	0.60	9000	8850

"Number-average degree of polymerization (DP) of PDMS bottlebrush backbone ($n_{\rm bb}$) determined by $^1{\rm H}$ NMR. $^b{\rm Number-average}$ DP of each PMMA linear block ($n_{\rm L}$) determined by $^1{\rm H}$ NMR, $^c{\rm Volume}$ fraction of L-blocks was calculated using mass densities $\rho_{\rm PMMA}=1.15$ g/mL and $\rho_{\rm PDMS}=0.96$ g/mL. $^d{\rm Elongation}$ range used for fitting (Figure 3c). $^e{\rm Structural}$ modulus and $^f{\rm Strain}$ -stiffening parameter are fitting parameters in eq 2. $^g{\rm Young's}$ modulus determined from eq 4 and $^h{\rm from}$ the tangent of a stress–strain curve at $\lambda=1$.

plastomer 900-1 demonstrated a remarkable areal strain of $\lambda_{\rm a}$ = 5 (Figure 3d and Movie S1) that surpasses conventionally prestrained silicone and acrylic materials. Polar Importantly, all samples do not exhibit an EMI, such as in bottlebrush elastomers, and instead are limited by MBD prior to the theoretical EBD. Therefore, additional fine-tuning of bottlebrush plastomer parameters ($n_{\rm bb}$, $n_{\rm sc}$, $n_{\rm gr}$, $n_{\rm L}$) will allow programming desired mechanical properties (i.e., extensibility) without sacrificing electroactuation capabilities. These materials are the first of their kind to achieve a combination of EMI-free tissue relevant softness due to their enhanced strain-stiffening.

EMI-free actuation of these materials also enables predictable reversibility. A plastomer actuator under sequential cyclic voltage (0–8.35 V/ μ m) below the calculated EBD (~11 $V/\mu m$) shows excellent reversibility with minimal hysteresis (<20%) at the highest strains (>80% breakdown strain) (Figures 3e, f). It should be noted that conventional elastomers show $\lambda_a^{\rm EMI} = 1.59$; bottlebrush elastomers show $\lambda_a^{\rm EMI} \cong 1.6$, ¹⁴ and bottlebrush plastomers demonstrate controlled reversibility to unprecedented $\lambda_a \cong 1.97$. It is also worth mentioning that the induced strain rate from the applied electrical field is ca. $0.024~\mbox{s}^{-1}$, which is close to the upper level of quasi-static tests.³⁰ After three cycles, voltage was increased to rupture at 10.34 V/ μ m and $\lambda_a^{BD} \cong 2.4$ consistent with a noncycled fresh film. This reversible actuation is a result of plastomer elasticity, before viscoelastic linear block yielding, as verified by cyclic uniaxial extension-compression cycles (Figure 3e). However, even in the full strain regime, minimal hysteresis is observed (<10%). As these materials require no solvent, they are immune to either aging under extreme environments or fatigue from extensive cycles and preform predictably until rupture, all of which is essential for the longevity of future actuators in biomedical or soft robotics fields. It should be noted the fatigue and failure of extended actuation cycles (>3) has not been presently demonstrated and will be the focus of future studies.

In summary, we introduce a new materials design platform for DEA applications via bottlebrush plastomers, which demonstrate a unique combination of properties including: (i) biologically relevant supersoftness with the Young's modulus in the kPa range, which enables both low-voltage operation and the integration of mechanically active components, (ii) inherent tissue-like strain-stiffening, which eliminates EMI without requiring film prestretch, (iii) high stretchability allowing large strokes, which expand their

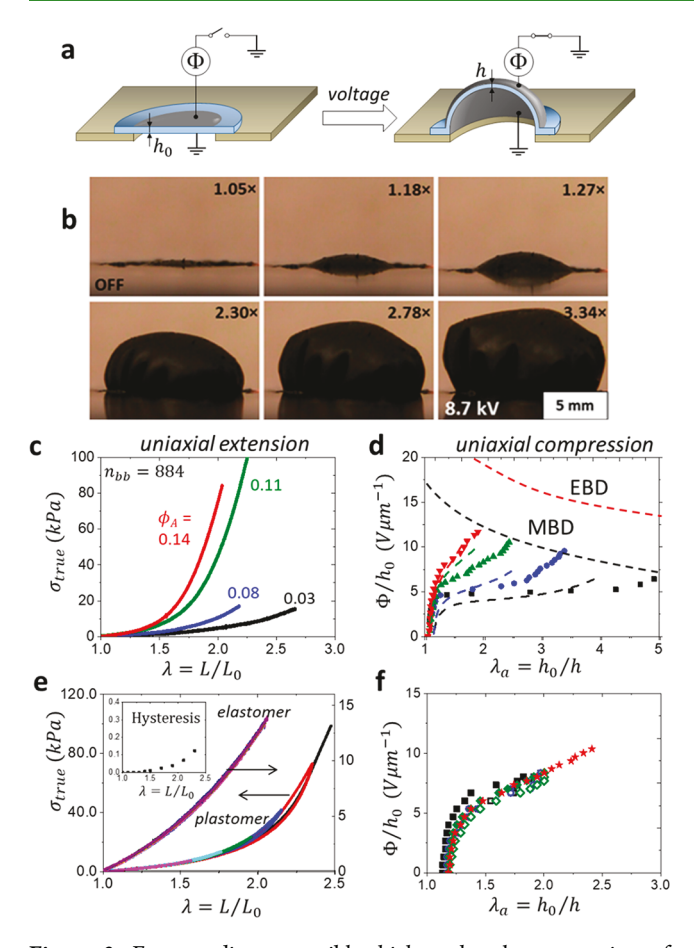


Figure 3. Free-standing, reversible, high-stroke electroactuation of biologically soft-yet-firm plastomers without electromechanical instability. (a) Freestanding circular DE diaphragm actuator of (b) a plastomer (sample 900-2) being subjected to an electrostatic field (Φ) at various areal extensibilities given in the picture insets. Given the isochoric nature of this process, the uniaxial compression from h_0 to h yields areal expansion $\lambda_a = A/A_0 = h_0/h$. The maximum areal expansion achieved for this sample was $\lambda_a = 3.34$. Irregularity in the actuated film is a result of uneven application of carbon grease electrodes and nonuniformity in the casted film thickness. (c) True stress $\sigma_{\rm true}$ as a function of uniaxial elongation $\lambda = L/L_0$ for four plastomers with $n_{\rm bb}$ = 884 and different $\phi_{\rm L}$ (Table 1). (d) All four plastomers avoid electromechanical instability (EMI) and are limited only by MBD, which occurs prior to EBD. The maximum strain generated in the diaphragm, $\varepsilon_a = (\lambda_a - 1)100\% = 400 \pm 50\%$, was achieved for the softest plastomer with $\phi_A = 0.03$ (Supplementary Movie S1). The dashed lines are calculated from the corresponding stress-strain curves in c. (e) Loading-unloading tensile cycles of a bottlebrush plastomer ($n_{\rm sc}$ = 14, $n_{\rm bb}$ = 1065, $\phi_{\rm A}$ = 0.13) reveal minimal (<10%) hysteresis emerging approximately halfway before rupture at $\lambda\cong 1.8$, as shown by increasing λ_{\max} : 1.6 (magenta), 1.75 (cyan), 1.9 (green), 2.15 (blue), and 2.35 (red). Inset: Hysteresis energy, normalized to the area under the corresponding stress-strain curve, as a function of λ shows relatively small hysteresis (<20%). (f) The 900-3 sample (Table 1) went under cyclic voltage (0-8.35 V/ μ m, >75% EBD) to examine the reversibility of the plastomer actuator. For this sample, $\lambda_a^{\rm BD} \cong 2.4$, and 8.35 V/ μ m is inducing $\lambda_a \cong 1.97$ which is >80% of $\lambda_a^{\rm BD}$. Filled and open symbols correspond to voltage increase and decrease, respectively, for four consecutive cycles: squares 1st, circles 2nd, rhombs 3rd, and stars 4th, respectively.

working range, (iv) high elasticity with low hysteresis enabling fully reversable strokes, (v) solvent-free compositions, which eliminate solvent leaching during operation to enhance DEA long-term stability in harsh environments (e.g., subterranean, deep sea, desert, and outer space), and (vi) are self-assembling physical networks that possess substantial potential for selfhealing, additive manufacturing, and reversible molding. Further, because molecular architecture largely determines the mechanical properties of thes systems, chemical composition can be leveraged to independently tailor application-specific characteristics, including biocompatibility, degradability, dielectric permittivity, and adhesion. Actuation was enabled without film prestretching and using relatively thick samples ($h_0 \cong 1 \text{ mm}$) at a low applied field ($\sim 1 \text{ V } \mu\text{m}^{-1}$), which suggests feasibility of achieving 10 V actuation for thinner films (\sim 10 μ m). Currently, mechanically robust films with a thickness of 200 μ m are readily prepared; enhancing the strength of our materials up to 10 MPa through future studies of a graft block copolymer architecture would enable reaching the desired 10 μ m range. We hope that future work will adapt this platform to various chemistries to realize these distinct potentials in soft robot applications such as biomedical implants, artificial muscles, haptic displays, and soft robotic

ASSOCIATED CONTENT

Supporting Information

The Supporting Information is available free of charge at https://pubs.acs.org/doi/10.1021/acsapm.0c00141.

Electroactuation of a freestanding circular diaphragm (MP4)

S1, synthesis and molecular characterization of bottlebrush thermoplastic elastomers; S2, physical characterization of mechanical and electric properties (PDF)

AUTHOR INFORMATION

Corresponding Authors

Sergei S. Sheiko — Department of Chemistry, University of North Carolina, Chapel Hill, North Carolina 27599-3290, United States; oorcid.org/0000-0003-3672-1611; Email: sergei@email.unc.edu

Mohammad Vatankhah-Varnosfaderani — Department of Chemistry, University of North Carolina, Chapel Hill, North Carolina 27599-3290, United States; ⊙ orcid.org/0000-0001-7636-9099; Email: mvatan@live.unc.edu

Authors

Vahid Karimkhani — Department of Chemistry, University of North Carolina, Chapel Hill, North Carolina 27599-3290, United States; oorcid.org/0000-0003-0668-8814

Andrew N. Keith — Department of Chemistry, University of North Carolina, Chapel Hill, North Carolina 27599-3290, United States; Occid.org/0000-0001-6351-5392

Erfan Dashtimoghadam — Department of Chemistry, University of North Carolina, Chapel Hill, North Carolina 27599-3290, United States; Oorcid.org/0000-0001-5607-7961

Benjamin J. Morgan — Department of Chemistry, University of North Carolina, Chapel Hill, North Carolina 27599-3290, United States; Occid.org/0000-0002-2925-5029

Michael Jacobs — Department of Polymer Science, University of Akron, Akron, Ohio 44325, United States; orcid.org/0000-0002-7255-3451

Andrey V. Dobrynin — Department of Polymer Science, University of Akron, Akron, Ohio 44325, United States; oorcid.org/0000-0002-6484-7409 Complete contact information is available at: https://pubs.acs.org/10.1021/acsapm.0c00141

Funding

The National Science Foundation (DMR 1407645, DMR 1535412, DMR 1921835, and DMR 1921923) and the Advanced Energy Consortium (subaward BEG 10-06)

Notes

The authors declare no competing financial interest.

ACKNOWLEDGMENTS

The authors gratefully acknowledge funding from the National Science Foundation (DMR 1407645, DMR 1535412, DMR 1921835, and DMR 1921923) and the Advanced Energy Consortium (subaward BEG 10-06).

REFERENCES

- (1) Trivedi, D.; Rahn, C. D.; Kier, W. M.; Walker, I. D. Soft Robotics: Biological Inspiration, State of the Art, and Future Research. *Applied bionics and biomechanics* **2008**, *5*, 99–117.
- (2) Ashley, S. Artificial Muscles. Sci. Am. 2003, 289, 52-59.
- (3) Acome, E.; Mitchell, S.; Morrissey, T.; Emmett, M.; Benjamin, C.; King, M.; Radakovitz, M.; Keplinger, C. Hydraulically Amplified Self-Healing Electrostatic Actuators with Muscle-Like Performance. *Science* **2018**, 359, 61–65.
- (4) Goh, Y. F.; Akbari, S.; Khanh Vo, T. V.; Koh, S. J. A. Electrically-Induced Actuation of Acrylic-Based Dielectric Elastomers in Excess of 500% Strain. *Soft robotics* **2018**, *5*, 675–684.
- (5) Rus, D.; Tolley, M. T. Design, fabrication and control of soft robots. *Nature* **2015**, *521* (7553), 467–475.
- (6) Whitesides, G. M. Soft Robotics. Angew. Chem., Int. Ed. 2018, 57, 4258-4273.
- (7) Mirvakili, S. M.; Hunter, I. W. Artificial Muscles: Mechanisms, Applications, and Challenges. *Adv. Mater.* **2018**, *30*, 1704407.
- (8) Mirfakhrai, T.; Madden, J. D.; Baughman, R. H. Polymer Artificial Muscles. *Mater. Today* **200**7, *10*, 30–38.
- (9) Brochu, P.; Pei, Q. Advances in Dielectric Elastomers for Actuators and Artificial Muscles. *Macromol. Rapid Commun.* **2010**, *31*, 10–36
- (10) Zhao, X.; Hong, W.; Suo, Z. Electromechanical Hysteresis and Coexistent States in Dielectric Elastomers. *Phys. Rev. B: Condens. Matter Mater. Phys.* **2007**, *76*, 134113.
- (11) Zhao, X.; Suo, Z. Theory of Dielectric Elastomers Capable of Giant Deformation of Actuation. *Phys. Rev. Lett.* **2010**, *104*, 178302.
- (12) Liang, H.; Sheiko, S. S.; Dobrynin, A. V. Supersoft and Hyperelastic Polymer Networks with Brushlike Strands. *Macromolecules* **2018**, *51*, 638–645.
- (13) Sheiko, S. S.; Dobrynin, A. V. Architectural Code for Rubber Elasticity: From Supersoft to Superfirm Materials. *Macromolecules* **2019**, *52*, 7531–7546.
- (14) Vatankhah-Varnoosfaderani, M.; Daniel, W. F.; Zhushma, A. P.; Li, Q.; Morgan, B. J.; Matyjaszewski, K.; Armstrong, D. P.; Spontak, R. J.; Dobrynin, A. V.; Sheiko, S. S. Bottlebrush elastomers: A New Platform for Freestanding Electroactuation. *Adv. Mater.* **2017**, *29*, 1604209.
- (15) Keith, A. N.; Vatankhah-Varnosfaderani, M.; Clair, C.; Fahimipour, F.; Dashtimoghadam, E.; Lallam, A.; Sztucki, M.; Ivanov, D. A.; Liang, H.; Dobrynin, A. V. Bottlebrush Bridge between Soft Gels and Firm Tissues. *ACS Cent. Sci.* **2020**, *6*, 413–419.
- (16) Treloar, L. R. G. The Physics of Rubber Elasticity; Oxford University Press, United States, 1975.
- (17) Keplinger, C.; Kaltenbrunner, M.; Arnold, N.; Bauer, S. Röntgen's Electrode-Free Elastomer Actuators Without Electromechanical Pull-in Instability. *Proc. Natl. Acad. Sci. U. S. A.* **2010**, 107, 4505–4510.

- (18) Keplinger, C.; Li, T.; Baumgartner, R.; Suo, Z.; Bauer, S. Harnessing SnapTthrough Instability in Soft Dielectrics to Achieve Giant Voltage-Triggered Deformation. *Soft Matter* **2012**, *8*, 285–288.
- (19) Thangawng, A. L.; Ruoff, R. S.; Swartz, M. A.; Glucksberg, M. R. An Ultra-Thin PDMS Membrane as a Bio/Micro-Nano Interface: Fabrication and Characterization. *Biomed. Microdevices* **2007**, *9*, 587–595.
- (20) Poulin, A.; Rosset, S.; Shea, H. R. Printing Low-Voltage Dielectric Elastomer Actuators. *Appl. Phys. Lett.* **2015**, *107*, 244104.
- (21) Madsen, F. B.; Daugaard, A. E.; Hvilsted, S.; Skov, A. L. The Current State of Silicone-Based Dielectric Elastomer Transducers. *Macromol. Rapid Commun.* **2016**, *37*, 378–413.
- (22) Vargantwar, P. H.; Özçam, A. E.; Ghosh, T. K.; Spontak, R. J. Prestrain-Free Dielectric Elastomers Based on Acrylic Thermoplastic Elastomer Gels: A Morphological and (Electro) Mechanical Property Study. *Adv. Funct. Mater.* **2012**, *22*, 2100–2113.
- (23) Niu, X.; Stoyanov, H.; Hu, W.; Leo, R.; Brochu, P.; Pei, Q. Synthesizing a New Dielectric Elastomer Exhibiting Large Actuation Strain and Suppressed Electromechanical Instability Without Prestretching. J. Polym. Sci., Part B: Polym. Phys. 2013, 51, 197–206. (24) Miriyev, A.; Stack, K.; Lipson, H. Soft Material for Soft Actuators. Nat. Commun. 2017, 8, 596.
- (25) Haines, C. S.; Li, N.; Spinks, G. M.; Aliev, A. E.; Di, J.; Baughman, R. H. New Twist on Artificial Muscles. *Proc. Natl. Acad. Sci. U. S. A.* **2016**, *113*, 11709–11716.
- (26) Vatankhah-Varnosfaderani, M.; Daniel, W. F.; Everhart, M. H.; Pandya, A. A.; Liang, H.; Matyjaszewski, K.; Dobrynin, A. V.; Sheiko, S. S. Mimicking Biological Stress—Strain Behaviour with Synthetic Elastomers. *Nature* **2017**, *549*, 497—501.
- (27) Vatankhah-Varnosfaderani, M.; Keith, A. N.; Cong, Y.; Liang, H.; Rosenthal, M.; Sztucki, M.; Clair, C.; Magonov, S.; Ivanov, D. A.; Dobrynin, A. V. Chameleon-Like Elastomers with Molecularly Encoded Strain-Adaptive Stiffening and Coloration. *Science* **2018**, 359, 1509–1513.
- (28) Mao, J.; Li, T.; Luo, Y. Significantly Improved Electromechanical Performance of Dielectric Elastomers via Alkyl Side-Chain Engineering. *J. Mater. Chem. C* **2017**, *5*, 6834–6841.
- (29) Clair, C.; Lallam, A.; Rosenthal, M.; Sztucki, M.; Vatankhah-Varnosfaderani, M.; Keith, A. N.; Cong, Y.; Liang, H.; Dobrynin, A. V.; Sheiko, S. S. Strained Bottlebrushes in Super-Soft Physical Networks. *ACS Macro Lett.* **2019**, *8*, 530–534.
- (30) Siviour, C. R. In High Strain Rate Characterization of Polymers. AIP Conference Proceedings; AIP Publishing: 2017, p 060029.